Enhanced Thermal Stability of Dipole Alignment in Inorganic–Organic Hybrid Films Containing Benzothiazole Chromophore

ARTICLE *in* THE JOURNAL OF PHYSICAL CHEMISTRY B · APRIL 2006

Impact Factor: 3.3 · DOI: 10.1021/jp057146a · Source: PubMed

6 AUTHORS, INCLUDING:

Yuanjing Cui
Zhejiang University
117 PUBLICATIONS **3,674** CITATIONS
SEE PROFILE

Zhiyu Wang
Zhejiang University
163 PUBLICATIONS **1,962** CITATIONS
SEE PROFILE

Junkuo Gao
Zhejiang Sci-Tech University
59 PUBLICATIONS **1,244** CITATIONS
SEE PROFILE

Enhanced Thermal Stability of Dipole Alignment in Inorganic−Organic Hybrid Films Containing Benzothiazole Chromophore

Yuanjing Cui, Guodong Qian,* Lujian Chen, Zhiyu Wang,* Junkuo Gao, and Minquan Wang

Department of Materials Science and Engineering, State Key Lab of Silicon Materials, Zhejiang University, Hangzhou 310027, PR China

Received: December 8, 2005; In Final Form: January 11, 2006

A new thermally stable second-order nonlinear optical (NLO) inorganic−organic hybrid film was successfully prepared by using a sol−gel process of alkoxysilane dye containing a benzothiazole unit. The dye-bonded precursor was synthesized from 3-isocyanatopropyltriethoxysilane and the heterocycle azo dye 2-[4′-(*N*-ethyl-*N*-2-hydroxyethyl)-amino-phenylazo]-6-nitrobenzothiazole (EHNBT) via a urethane reaction. Molecular structural characterization for the resultant was achieved by elemental analysis, FTIR, UV−visible spectra, and ^{1}H NMR. The second harmonic coefficients (d_{33}) of poled hybrid films measured by a Maker fringe technique were in the range 15.9−72.1 pm/V at a wavelength of 1064 nm, depending on the concentration of alkoxysilane dye. The hybrid films containing the benzothiazole moiety exhibited higher thermal stability of dipole alignment at elevated temperatures than their analogues with a benzene ring. The d_{33} value of the poled film remained at 94% of its initial value after heating at 120 °C for 6 h, and only 18% decayed in 15 min at 180 °C. The result indicates that the hybrid film is suitable for the fabrication of an electro-optic device.

Introduction

Nonlinear optical (NLO) materials have been researched extensively since two decades ago because of their tremendous potential applications in the fields of optical information processing, optical sensing, data storage, and telecommunications.[1−3] The development of poled polymer thin films that are suitable for the fabrication of high-performance integrated optical devices is presently a major focus of research in second-order nonlinear optics.[4−6] Compared to traditional inorganic crystals, poled polymers offer many advantages such as greater NLO activity, an intrinsic low dielectric constant, and an ultrafast response. In recent years, numerous poled polymers have been synthesized as NLO media, and a few devices with large optical nonlinearity have been demonstrated.[7−10] However, because of the rotational freedom of the chromophores and the motion of polymer chains, the second-order nonlinear optical properties are thermodynamically unstable, especially at higher temperatures. The thermal stability of poling-induced chromophore dipole alignment has been one of the major problems that prevent the application of those materials for actual devices.

Various approaches for higher thermal stability have been investigated including the cross-linking after aligning the dipole as well as the use of the highly rigid backbone etc.[11−13] From current literature, it appears that the sol−gel materials have received much attention and have been considered to be one of the most potential matrix candidates for stabilizing poled dipole orientation.[14,15] By incorporating the NLO active dyes into the inorganic silica network, the resulting inorganic−organic materials may display high optical transparency, good thermal stability, and excellent NLO properties. Moreover, the sol−gel matrix provides an inert environment for organic chromophores and theoretically will prevent damage induced by corona discharge poling and thermal decomposition.

Up to now, the main chromophores employed in inorganic−organic hybrid NLO materials are common push−pull type dyes with a benzene ring as the conjugating moiety. The most widely used azo dye Disperse Red 1 (DR1, *N*-ethyl-*N*-2-hydroxyethyl-*p*-nitrophenylazoaniline) is an example. However, the NLO properties concerning a heterocycle chromophore in sol−gel film is scarcely reported. Compared to the previous works, we decide to use a different chromophore that has a benzothiazole as the conjugating unit between donor and acceptor groups. The color chemistry studies have evidenced that the replacement of a benzene ring by a less aromatic heterocycle in a typical donor−acceptor molecule will reduce the charge-transfer transitional energy and result in a significant bathochromic shift of the visible absorption band due to the deficiency of electron density on the heterocycle C-atom.[16] This red shift of $\pi-\pi^*$ transition indicates that the heterocycle chromophore possess a larger molecular hyperpolarizability (β) than that of their benzenoid analogues, according to theoretical NLO studies.[17] In addition, replacement of a benzene ring in chromophores with a heterocycle has been shown to improve the thermal stability dramatically.[17]

In this paper, a new alkoxysilane dye (ASD) containing a benzothiazole unit was synthesized, and then a series of transparent inorganic−organic hybrid films were prepared from the resulting precursor via a sol−gel process, and the hybrid film containing a DR1 molecule was also prepared at the same condition as a reference. The chemical structure of the sol−gel precursor containing a chromophore was shown in Figure 1. The NLO properties and its thermal stability of the hybrid films containing a benzothiazole unit were discussed and compared with that of the benzenoid analogue. The aim is to investigate the effect of the structure of chromophores on NLO properties and its thermal stability of sol−gel hybrid films.

* Corresponding author. Telephone: +86-571-87952334. Fax: +86-571-87951234. E-mail address: gdqian@zju.edu.cn; wangzhiyu@zju.edu.cn.

10.1021/jp057146a CCC: $33.50
Published on Web 02/04/2006

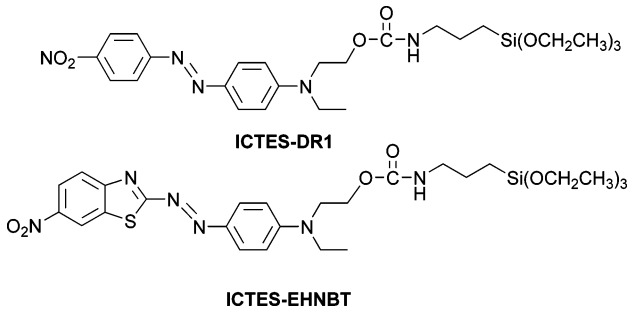

Figure 1. Chemical structure of alkoxysilane dyes investigated in this study.

Experimental Section

Materials. Tetrahydrofuran (THF) was dried by refluxing, distilling from calcium hydride just before use. 2-Amino-6-nitrobenzothiazole and 3-isocyanatopropyltriethoxysilane (ICPTEOS) were purchased from Tokyo Chemical Industry Co. and used as received. *N*-Ethyl-*N*-(2-hydroxyethyl)aniline was obtained from Acros and used without further purification. Other reagents and solvents, of analytical-grade quality, were commercial products and used as received.

Synthesis of 2-[4′-(*N*-Ethyl-*N*-2-hydroxyethyl)-amino-phenylazo]-6-nitrobenzothiazole (EHNBT).[18] 2-Amino-6-nitrobenzothiazole (7.8 g, 40 mmol) dissolved in 56 mL of a mixture of formic acid, propionic acid, phosphoric acid, and acetic acid (1:1:2:3) was cooled to 0−5 °C and then treated by adding dropwise a nitrosyl sulfuric acid solution which was prepared by slowly adding the sodium nitrite (2.8 g, 40 mmol) in small portions to 20 mL of concentrated (98%) sulfuric acid under stirring and cooling. After stirring for 1 h in an ice bath, *N*-ethyl-*N*-(2-hydroxyethyl)aniline (7.3 g, 44 mmol) in 120 mL of methanol/water (2/1, v/v) was added, then stirred for 1 h under cooling after complete addition, followed by neutralization (pH 5−6) with ammonia, and stirred for 2 h more. The precipitate was filtered off, washed by plenty of water, and purified by flash chromatography using cyclohexane/ethyl acetate (1/2, v/v), and then pure chromophore EHNBT was obtained as a black purple powder. Yield: 39%, mp 210 °C.

FTIR (KBr pellet, cm^{-1}): 3458 (−OH), 1600 ($-C_6H_4$), 1525 ($-NO_2$, ν_{as}), 1330 ($-NO_2$, ν_s). ^{1}H NMR (500 MHz, DMSO-d_6, ppm): 9.02 (d, Ar**H**, 1H), 8.29 (q, Ar**H**, 1H), 8.11 (d, Ar**H**, 1H), 7.88 (d, Ar**H**, 2H), 7.01 (d, Ar**H**, 2H), 4.94 (s, O**H**, 1H), 3.64 (t, C**H**$_2$, 6H), 1.20 (m, C**H**$_3$, 3H). Anal. Calcd for $C_{17}H_{17}N_5O_3S$ (371.4): C, 54.97; H, 4.61; N, 18.86. Found: C, 54.46; H, 4.59; N, 18.72.

Synthesis of Alkoxysilane Dye (ICPTEOS-EHNBT). A dry, 50 mL three-necked flask equipped with an oil bath, a mechanical stirrer, a nitrogen inlet, and a reflux condenser was charged with EHNBT (1.86 g, 5 mmol), 3-isocyanatopropyltriethoxysilane (ICPTEOS, 1.36 g, 5.5 mmol), 30 mL of THF and 5 drops of triethylamine (TEA) as catalyst. The reaction mixture was stirred and refluxed for 48 h under a nitrogen atmosphere. The compound was precipitated into dried hexane and collected by suction filtration. Yield: 69%, mp 123 °C.

FTIR (KBr pellet, cm^{-1}): 3389 (—NH), 1699 (−C═O), 1600 ($-C_6H_4$), 1527 ($-NO_2$, ν_{as}), 1335 ($-NO_2$, ν_s), 1105, 1079 (Si—O—CH_2CH_3). ^{1}H NMR (500 MHz, DMSO-d_6, ppm): 11.13 (s, N**H**, 1H), 9.04 (d, Ar**H**, 1H), 8.27 (q, Ar**H**, 1H), 8.14 (d, Ar**H**, 1H), 7.90 (d, Ar**H**, 2H), 7.03 (d, Ar**H**, 2H), 4.20 (s, $CH_2C\mathbf{H}_2O$, 2H), 3.76 (m, $OC\mathbf{H}_2CH_3$, 6H), 3.63 (d, $C\mathbf{H}_2CH_2O$, 2H), 3.16 (d, $C\mathbf{H}_2CH_3$, 2H), 2.26 (d, $C\mathbf{H}_2CH_2CH_2$, 2H), 1.53 (d, $CH_2C\mathbf{H}_2CH_2$, 2H), 1.15 (m, $CH_2C\mathbf{H}_3$, 12H), 0.59 (t, $CH_2C\mathbf{H}_2$, 2H). Anal. Calcd for $C_{27}H_{38}N_6O_7SSi$ (618.8): C, 52.41; H, 6.19; N, 13.58. Found: C, 52.55; H, 6.22; N, 13.70.

Synthesis of Alkoxysilane Dye (ICPTEOS-DR1). ICPTEOS-DR1 was synthesized and characterized as described in a previous paper.[19]

Preparation of Inorganic−Organic Hybrid Film. To prepare the coating solution, the alkoxysilane dye ICPTEOS-EHNBT was mixed with tetraethoxysilane (TEOS) at a 1:10, 1:5, 1:3, and 1:1 molar ratio, respectively, in THF. The molar ratio of ASD and TEOS will be noted in the parentheses when necessary. Then acidic water (HCl, pH = 1) was added, and the H_2O/Si molar ratio was 4:1. The solution was stirred for 6 h and aged at room temperature for 2 days to increase viscosity. The sol was filtered through a 0.22 μm Teflon membrane filter before spin coating on the indium−tin oxide (ITO) glass substrates. The coated films were dried in a vacuum oven at room temperature for 12 h to remove the residual solvent. Following the same procedure, the sol−gel film containing DR1 (1:3) was obtained.

Second Harmonic Generation (SHG) Measurement. The second-order optical nonlinearity of hybrid films was determined by in situ second harmonic generation (SHG) measurement. A closed temperature controlled oven having optical windows and equipped with tungsten needle electrodes was used. The film, which was kept at 45° to the incident beam, was poled inside the oven. The poling condition was as follows: voltage, 5.5 KV; gap distance, 1 cm. The laser source is a Q-switched Nd:YAG pulse laser with a 1064 nm fundamental beam (500mJ maximum energy, 3−5 ns pulse width, and 10 Hz repeating rate). The generated second harmonic wave was passed through a monochromator and detected by a photomultiplier. The signal was averaged on a Stanford Research Systems (SRS) model SR-250 gated integrator and boxcar averager module and transferred to a microcomputer through a computer interface module SR-254.

Characterization. FTIR spectra were recorded on a Nicolet Avatar 360 in the region of 4000−400 cm^{-1} using KBr pellets. ^{1}H NMR spectra were obtained with a Bruker Avance DMX500 spectrometer using tetramethysilane (TMS) as an internal reference. Elemental analysis was carried out on an Eager 300 microelemental analyzer. A UV−vis−NIR transmittance spectrum was measured using a Hitachi U-4100 spectrophotometer. A UV−vis absorption spectroscopic study was performed on a Perkin-Elmer Lambda 20 spectrophotometer. Differential scanning calorimetry (DSC) was performed using a Perkin-Elmer DSC-7 with a heating rate of 10 °C/min. Thermalgravimetric analysis (TGA) was performed with a Perkin-Elmer Pyris-1 thermogravimetric analyzer at 20 °C/min up to 600 °C under nitrogen atmosphere. The thickness of thin films was determined using the Metricon PC 2010 prism coupler.

Results and Discussion

Synthesis and Chemical Characterization. Molecular structures of hybrid film containing benzothiazole moiety and the synthetic route are shown in Scheme 1. The heterocyclic NLO chromophore was synthesized by a diazonium coupling reaction. Due to the weak basicity of 2-amino-6-nitrobenzothiazole and the protonation of the heterocycle N-atom in acid, the formation of stable diazonium salts is difficult.[18] In this study, the nitrosyl sulfuric acid was selected as a diazotizing agent because of its high reactivity, and various acids were used to increase the solubility of 2-amino-6-nitrobenzothiazole in the reaction medium. The resulting chromophore was further reacted with 3-isocyanatopropyl-triethoxysilane (ICPTEOS) in the presence

SCHEME 1. Synthetic Route of Hybrid Film Containing Benzothiazole Unit

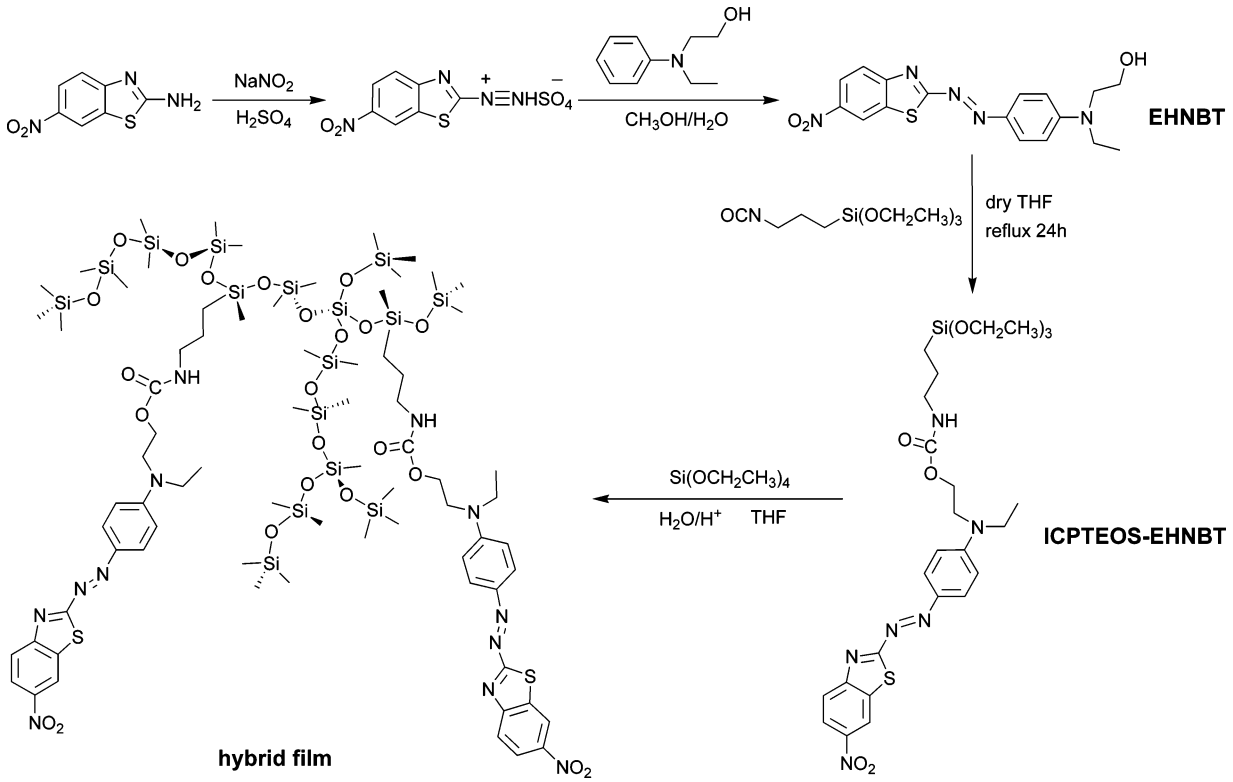

of triethylamine as catalyst to give the alkoxysilane dye (ICPTEOS-EHNBT) via a urethane forming reaction. The chemical structure of the product was confirmed by elemental analysis, FTIR, and ^{1}H NMR spectroscopy.

Through the hydrolysis and copolymerization process of a dye-bonded precursor with TEOS, various transparent and stable inorganic−organic hybrid films were prepared. The thickness of the films was in the range 0.7−1.1 μm. The addition of TEOS was intended to increase the cross-linking density of the silica matrix. The spin-coated hybrid films are tough and resistant to organic solvents. After drying under vacuum, the films were soaked in THF which is a good solvent for the alkoxysilane dye, the solvent did not extract any measurable concentration of the dye from the films, indicating that the chromophore has been firmly incorporated into the silica matrix.

The FTIR spectra of chromophore, alkoxysilane dye, and film are shown in Figure 2. In the IR spectra of the chromophore, the absorption bands at 3458, 1600, and 1525 cm^{-1} were attributed to the stretching vibration of the hydroxyl, benzene ring, and nitro group, respectively. In the spectra of the alkoxysilane dye, the absorption bands at 1600 and 1525 cm^{-1} exhibited no significant change, while the absorption band at 3458 cm^{-1} disappeared, and new absorption bands at 3389 and 1699 cm^{-1} appeared, contributed by the amino and carbonyl stretching vibration of the carbamate. In addition, a new absorption band due to the Si−O−C_2H_5 group emerged at 1079 cm^{-1}. In the spectra of films, a large absorption band between 1200 and 1000 cm^{-1} due to the Si−O−Si stretching was observed, indicating that the dye-attached precursor has hydrolyzed and polymerized.

The thermal stability of the hybrid film and chromophore was determined by thermogravimetric analysis (TGA) under atmosphere (see Figure 3). The initial decomposition temperature of the hybrid film (1:3) is 252 °C, higher than that of the chromophore. This result indicates that the covalent linkage between the chromophore and silica matrix could prevent the decomposition of the chromophore. No clear glass transition temperature (T_g) could be observed up to 300 °C in the DSC measurement of the hybrid film. It means that the hybrid film should have a higher T_g due to its high cross-linking silicon−oxygen network.

NLO Properties. The UV−vis−NIR transmittance of the hybrid films containing DR1 and EHNBT were measured in the wavelength range 400−2500 nm. From the spectrum (Figure 4), it is noted that the transparency cutoff occurs around 600 nm which can be attributed to the absorption of chromophores. Further, there is no undesirable absorption in the spectra, and the transmittance is 95−98% from 700 to 2500 nm, which is good enough for the application of electro-optic modulation using a diode laser.

Figure 5 shows the UV−visible spectra of a hybrid film containing EHNBT (1:3) before and after poling. Generally, azo dyes exhibit a low-intensity $n-\pi^*$ band in the visible region of

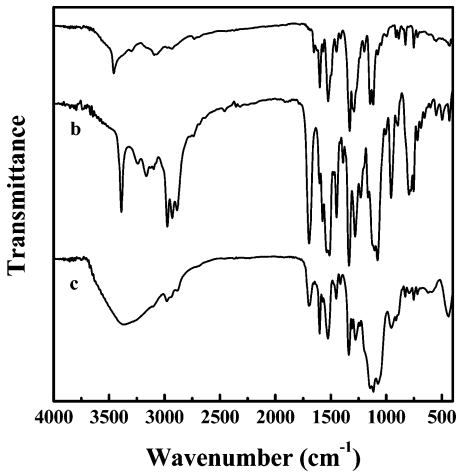

Figure 2. FTIR spectra of EHNBT (a), ICPTEOS-EHNBT (b), and hybrid film (c).

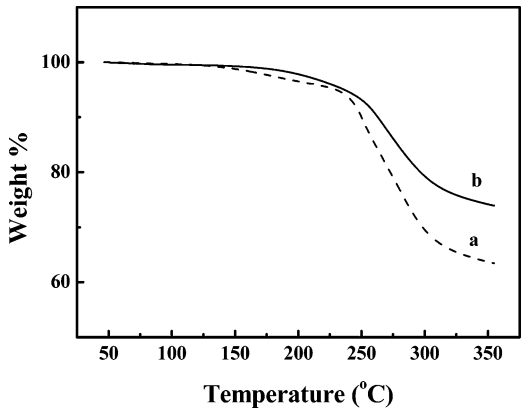

Figure 3. TGA traces for chromophore EHNBT (a) and hybrid film containing EHNBT (b).

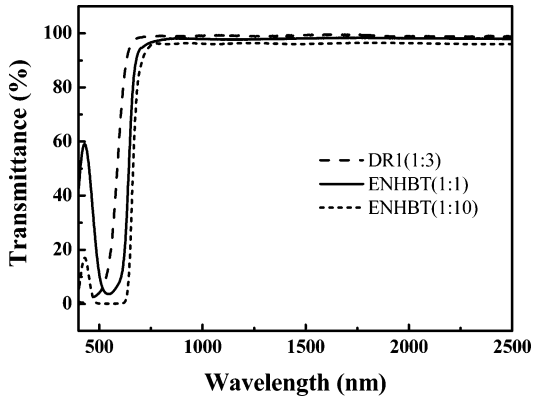

Figure 4. Optical transmittance spectrum of hybrid films containing DR1 and EHNBT.

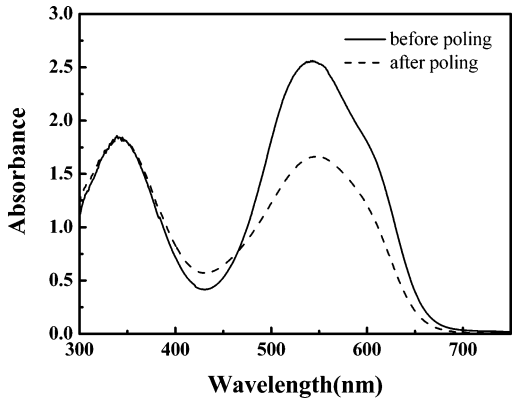

Figure 5. UV−vis absorption spectra of hybrid film (1:3) before and after poling.

the spectrum and a high-intensity $\pi-\pi^*$ band in the UV region. Substitution with a strong electron donor and electron acceptor, such as the benzothiazole chromophore investigated here, effectively reduces the charge-transfer transitional energy of the $\pi-\pi^*$ transition. Therefore, the corresponding band is batho-chromically shifted and overlaps the weak $n-\pi^*$ band. As seen in Figure 5, the hybrid films exhibited strong absorption bands in the visible region with maxima (λ_{max}) at about 542 nm. To evaluate the noncentrosymmetric alignment of the chromophores in hybrid films, the absorption spectra of hybrid film before and after poling were compared. Poling causes a decrease of absorption intensity and a red shift of the absorption peak. The order parameter ϕ ($\phi = 1 - A_1/A_0$; A_0 and A_1 are absorbance of the film before and after poling) was used to characterize the poling efficiency.[20] Under the condition of a 5.5 kV poling

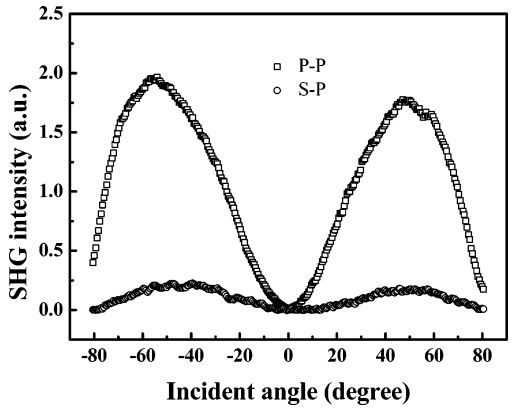

Figure 6. Angular dependence of SHG intensity in a poled hybrid film.

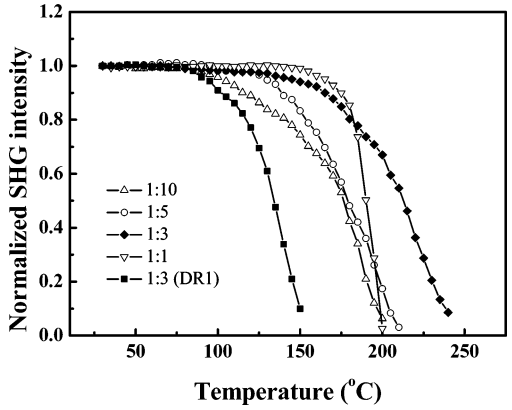

Figure 7. Decay of the SHG signal as a function of temperature for the films containing EHNBT and a referenced film containing DR1.

voltage applied to the corona needle at 160 °C for 1 h, the order parameter value for hybrid film containing EHNBT (1:3) was calculated to be 0.36. In the same way, we obtained the order parameter values 0.35, 0.33, and 0.36 for the film with molar ratios 1:10, 1:5, and 1:1, respectively. The order parameter value of film containing DR1 (1:3) was also determined to be 0.34, which is near that of the films with EHNBT.

The second-order NLO properties of the hybrid films were characterized by SHG measurement using the Maker fringe technique. The typical Maker fringe pattern of the poled film (1:3) is shown in Figure 6. The second harmonic coefficient (d_{33}) of hybrid film can be calculated by comparison with the SHG intensity of a standard Y-cut quartz crystal plate.[21−24] From the calculation, we obtained the d_{33} values 15.9, 29.9, 45.5, and 72.1 pm/V for the films with molar ratios 1:10, 1:5, 1:3, and 1:1, respectively, after poling at 160 °C for 1 h. The d_{33} value of film containing DR1 was also determined to be 32.4 pm/V.

As far as NLO devices are concerned, the thermal stability of the poled films is of paramount importance. The stability of optical nonlinearity was studied both by dynamic stability measurements and by isothermal decay measurements. The dynamic thermal stability of the SHG signal was investigated through a depoling experiment in which the SHG signal was monitored as the poled film was heated at a rate of 10 °C/min from 30 to 250 °C. Figure 7 shows the results of the hybrid films containing a benzothiazole moiety and a referenced sample containing DR1. It indicates that the hybrid film with the heterocycle unit has a higher thermal stability of dipole alignment than its benzenoid analogue. In these sol−gel films,

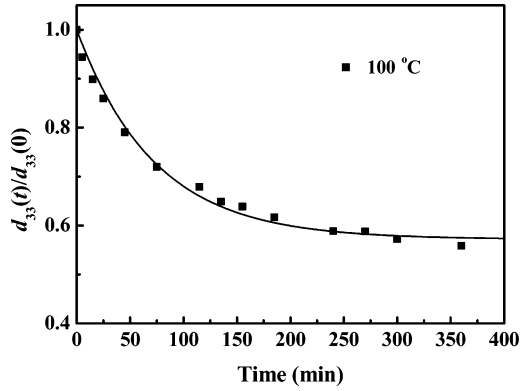

Figure 8. Temporal stability of the normalized d_{33} of hybrid film containing DR1 (1:3) at 100 °C.

the NLO molecules are attached to the silica backbone as a side pendant. The free volume of the network is sufficient to allow reorientation of the chromophores after poling because of the large size of the siloxane linkage and the propyl chain. Therefore, it is expected that the smaller free volume between the NLO molecules and matrix should enhance the thermal stability of the poled alignment. Using Chemoffice software, the radius of the chromophore EHNBT and DR1 were calculated to be 0.8 and 0.6 nm, respectively. Thus, the smaller free volume of the films containing a benzothiazole chromophore significantly contributes to the restriction of molecular motion in silica matrix.

For the same reason, the thermal stability of NLO properties for the heterocycle films increase with increasing the concentration of chromophores. The film (1:1) has a highest decay onset temperature at 170 °C, but the SHG signal rapidly vanishes around 200 °C. This decrease could be attributed to the decomposition of residual alkoxysilane dyes due to its relative high content. The poled film (1:3) also exhibited excellent thermal stability, and there was little decay of the SHG signal below 130 °C, as shown in Figure 7. Up to 90% of the nonlinearity remained at 165 °C, and approximately 50% of SHG signal remained even at 215 °C, which is 80 °C higher than that of the film containing DR1. All the results indicate that the optimal molar ratio of chromophore and TEOS at which the NLO properties, optical transparency, and thermal stability of the hybrid films perform best is 1:3.

To further understand the thermal behavior of the hybrid film, isothermal decay was performed. Figure 8 shows the $d_{33}(t)/d_{33}(0)$ value of hybrid film containing DR1 (1:3) as a function of time at 100 °C, where $d_{33}(t)$ and $d_{33}(0)$ represent the second harmonic coefficient at time t and time 0, respectively. It can be seen that the optical nonlinearity of the hybrid film significantly decreased; after 6 h at a temperature of 100 °C, only 56% of initial d_{33} value remained. However, the film containing EHNBT (1:3) displayed higher thermal stability. The heterocycle film was heated to 120 °C and 180 °C, respectively, and the variations of the normalized d_{33} value were shown in Figure 9. We could observe a slow decay of $d_{33}(t)/d_{33}(0)$ value at a temperature of 120 °C, and the normalized d_{33} value did not significantly change after 6 h, which finally stabilized around 94% of the initial value. Even at 180 °C, only 18% of the d_{33} value decreased after 15 min.

It is clear that the relaxation of the dipole alignment in the heterocycle films is less than that of the conventional side-chain NLO polymer due to the large molecular size. Generally, such high thermal stability is expected to be found in main-chain polymers or cross-linked polyimide materials. The decay curves

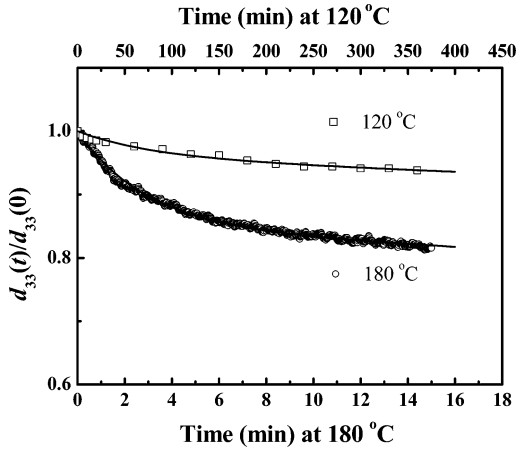

Figure 9. Temporal stability of the normalized d_{33} of hybrid film containing EHNBT (1:3) at 120 °C and 180 °C.

TABLE 1: Parameters for the Relaxation of the SHG Intensity at 120 °C and 180 °C

temp (°C)	A	τ_1 (min)	τ_2 (min)
120	0.04	79.3 ± 1.56	15 474.8 ± 14.82
180	0.15	2.92 ± 0.01	400.9 ± 2.70

of d_{33} can be fitted to a biexponential function,[25]

$$\frac{d_{33}(t)}{d_{33}(0)} = A\exp\left(-\frac{t}{\tau_1}\right) + (1-A)\exp\left(-\frac{t}{\tau_2}\right) \quad (1)$$

where A is the amplitude of the rapid decay regime, and τ_1 and τ_2 are the time constants characterizing the rapid and slow decay of chromophore orientation in the matrix, respectively. The A value and relaxation times τ_1 and τ_2 were calculated and presented in Table 1. It was found that the parameter A increases and τ_1 and τ_2 values decrease with increasing annealing temperature.

The relaxation time can be expressed by the Arrhenius equation,[26]

$$\tau = \tau_0 \exp\left(\frac{Q}{KT}\right) \quad (2)$$

where Q is the activation energy, K is the Boltzmann constant, and T is the temperature. Fitting the τ_2 values at various temperatures on the equation, Q and τ_0 are calculated to be 0.94 eV and 1.6×10^{-8} min, respectively. Using extrapolation to room temperature of the Arrhenius equation, the slow relaxation time τ_2 is estimated to be 346 years. This result implies a long-term stability of the nonlinearity for the hybrid film at room temperature.

Conclusions

In conclusion, a new class of inorganic−organic hybrid films containing a benzothiazole moiety in the side chain were prepared by a sol−gel technique. SHG measurement indicated that the second harmonic coefficients (d_{33}) of hybrid films were in the range 15.9−72.1 pm/V at 1064 nm, which is larger than the d_{33} value of the analogous film containing DR1. The poled films also exhibited higher temporal and thermal stability of nonlinearity than their benzenoid analogues due to the smaller free volume in the silica network. These properties are better than that of the conventional side-chain NLO materials and are comparable with that of the cross-linked polyimide materials

or main-chain polymers. It indicates that the film can meet the long-term stability requirement for optical components.

Acknowledgment. The authors gratefully acknowledge the financial support for this work from the National Natural Science Foundation of China (under Grant No. 50532030) and the Foundation for the Author of National Excellent Doctoral Dissertation of P. R. China (No. 200134).

References and Notes

(1) Ermer, S.; Valley, J. F.; Lytel, R.; Lipscomb, G. F.; Vaneck, T. E.; Girton, D, G. *Appl. Phys. Lett.* **1992**, *61*, 2272.

(2) Zyss, J. *Molecular Nonlinear Optics Materials Physics and Devices*; Academic Press: Orlando, FL, 1994.

(3) Prasad, P. N.; Williams, D. J. *Introduction to Nonlinear Optical Effects in Molecules and Polymers*; John Wiley & Sons, Inc.: New York, 1991.

(4) Dolton, L. R. *Chem. Ind.* **1997**, *7*, 510.

(5) Marder, S. R.; Kippelen, B.; Jen, A. K.-Y.; Peyghambarian. *Nature* **1997**, *388*, 845.

(6) Krgal, H.; Hohmann, R.; Marheine, C.; Pott, W.; Pompe, G.; Neyer, A.; Diepold, T.; Obermeier, E. *Electron. Lett.* **1998**, *34*, 1396.

(7) Sandhya, K. Y.; Pillai, C. K. S.; Tsutsumi, N. *Prog. Polym. Sci.* **2004**, *29*, 45.

(8) Lee, J. Y.; Bang, H. B.; Park, E. J.; Baek, C. S.; Rhee. B. K.; Lee, S. M. *Synthetic Metals* **2004**, *144*, 159.

(9) Jeng, R. J.; Hung, W. Y.; Chen, C. P.; Hsiue, G. H. *Polym. Adv. Technol.* **2003**, *14*, 66.

(10) Burzynski, R.; Cassterens, M. K.; Zhang, Y. *Opt. Eng.* **1996**, *35*, 443.

(11) Kim, T. D.; Lee, K. S.; Lee, G. U.; Kim, O. K. *Polymer* **2000**, *41*, 5237.

(12) Hwang, Y. H.; Kim, J. L.; Park, S. Y.; Hong, S. *Polymer Bulletin* **1999**, *42*, 175.

(13) Lu, Z. Q.; Shao, P.; Li, J.; Hua, J. L.; Qin, J. G.; Qin, A. J.; Ye, C. *Macromolecules* **2004**, *37*, 7089.

(14) Zhang, H. X.; Lu, D.; Fallahi, M. *Appl. Phys. Lett.* **2004**, *84*, 1064.

(15) Chaumel, F.; Jiang, H. W.; Kakkar, A. *Chem. Mater.* **2001**, *13*, 3389.

(16) Hallas, G.; Choi, J. H. *Dyes Pigm.* **1999**, *40*, 99.

(17) Ledoux, I.; Zyss, J.; Barni, E.; Barolo, C.; Diulgheroff, N.; Qualiotto, P.; Viscardi, G. *Synthetic Metals* **2000**, *115*, 213.

(18) Cojocariu, C.; Rochon, P. *J. Mater. Chem.* **2004**, *14*, 2909.

(19) Cui, Y. J.; Wang, M. Q.; Chen, L. J.; Qian, G. D. *Dyes Pigm.* **2004**, *62*, 43.

(20) Mortazavi, M. A.; Knoesen, A.; Kowel, S. T.; Higgins, B. G.; Dienes, A. *J. Opt. Soc. Am. B* **1989**, *6*, 733.

(21) Dalton, L. R.; Xu, C.; Harper, A. W.; Ghson, R.; Wu, B.; Liang, Z.; Montgomery, R.; Jen, A. K.-Y. *Nonlinear Opt.* **1995**, *10*, 383.

(22) Pan, Q. W.; Fang, C. S.; Qin, Z. H.; Gu, Q. T.; Cheng, X. F.; Xu, D.; Yu, J. Z. *Mater. Lett.* **2003**, *57*, 2612.

(23) Amano, M.; Kaino, T. *J. Appl. Phys.* **1990**, *68*, 6024.

(24) Luo, J. D.; Qin, J. G.; Kang, H.; Ye, C. *Chem. Mater.* **2001**, *13*, 927.

(25) Lebeau, B.; Brasselet, S.; Zyss, J.; Sanchez, C. *Chem. Mater.* **1997**, *9*, 1012.

(26) Goudket, H.; Canva, M.; Levy, Y.; Chaput, F.; Boilot, J. P. *J. Appl. Phys.* **2001**, *90*, 6044.